Proceedings of IMECE2006
2006 ASME International Mechanical Engineering Congress and Exposition
November 5-10, 2006, Chicago, Illinois, USA

IMECE2006-13417

ASSESSMENT OF RELEVANT PHYSICAL PHENOMENA CONTROLLING THERMAL PERFORMANCE OF NANOFLUIDS

M. Bahrami[1]
Deptartment of Mechanical Engineering,
University of Victoria, Victoria,
BC, V8W 3P6, Canada.

M. M. Yovanovich[2] and J. R. Culham[3]
Department of Mechanical Engineering,
University of Waterloo, Waterloo,
ON, N2L 3G1, Canada.

Abstract

This paper provides an overview of the important physical phenomena necessary for the determination of effective thermal conductivity of nanofluids. Through an investigation, a large degree of randomness and scatter has been observed in the experimental data published in the open literature. Given the inconsistency in the data, it is impossible to develop a comprehensive physical-based model that can predict all the trends. This also points out the need for a systematic approach in both experimental and theoretical studies.

Upper and lower bounds are developed for steady-state conduction in stationary nanofluids. Comparisons between these bounds and the experimental data indicate that all the data (except for carbon nanotube data) lie between the lower and upper bounds.

Nomenclature

a	=	basic cell half side, m
d_p	=	particle diameter, m
k	=	thermal conductivity, W/mK
Q	=	heat flow rate, W
r_p	=	particle radius, m
SSM	=	steady-state method
T	=	temperature, K
THW	=	transient hot wire
V	=	particle velocity, m/s
ϕ	=	volume fraction

Subscripts

e	=	effective
HC	=	Hamilton-Crosser
l	=	lower bound
m	=	matrix, base fluid
p	=	particle
u	=	upper bound

1 INTRODUCTION

The significant growth in performance and functionality of microelectronics combined with a miniaturization trend in Micro Electro Mechanical Systems (MEMS) have resulted in an unprecedented increase in heat loads that presents a great challenge to thermal engineers. Nanofluids show promise to meet these challenges.

Nanofluids, a name coined by Choi [1], are liquid-particle laden mixtures consisting of solid nanoparticles, with sizes less than 100 nm, suspended in a liquid, with solid volume fractions typically less than 4%. Pioneer works of Masuda et al. [2], Artus [3], and Eastman [4] introduced the thermal conductivity enhancement of nanofluids to the scientific community. Since then a large number of experimental and theoretical studies have been published by numerous research groups from all over the globe. This new class of heat transfer fluids has shown several attractive characteristics including the possibility of obtaining large enhancements (up to 40%) in thermal conductivity compared with the base liquid [5], strong temperature dependent effects [6], reduced friction coefficient [7], and significant increases (threefold) in critical heat flux [8]. Choi et al. [9] tested a carbon nanotube-in-oil nanofluid and reported a dramatic

[1]Assistant Professor. Corresponding author, E-mail: majid@mhtlab.uwaterloo.ca. Mem. ASME.
[2]Distinguished Professor Emeritus. Fellow ASME.
[3]Associate Professor. Director MHTL. Mem. ASME.

Copyright © 2006 by ASME

enhancement in the effective thermal conductivity of the nanofluid (factor of 2.5 at a volume fraction of 1%). Pak and Cho [10] studied the convective heat transfer coefficient of nanofluids in cylindrical tubes. They [10] used $\gamma-Al_2O_3$ and TiO_2 nanoparticles in water and showed that the Nusselt number of the nanofluid is higher than the base fluid. Furthermore, a new class of heat exchangers (using nanofluids) are being developed for medical applications including cancer therapy [11]. In addition, due to the small size of nanoparticles and small volume fraction, problems such as sedimentation, clogging, abrasion, and increase in pressure drop become insignificant. Observed behavior in many cases cannot be explained via existing macroscopic models, indicating the need for new models that properly capture the features of nanofluids.

Presently, there are two methods for fabricating nanofluids:

- *Two-step* process in which nanoparticles are first produced as a dry powder, typically by an inert gas–condensation method. The resulting nanoparticles are then dispersed into a fluid. This method may result in a large degree of nanoparticle agglomeration. On the other hand, the inert-gas condensation technique has already been scaled up to economically produce tonnage quantities of nanopowders [11].
- *Direct-evaporation* technique [12] (single-step), synthesizes nanoparticles and disperses them into a fluid in a single step. A significant limitation to the application of this technique is that the liquid must have low vapor pressure, typically less than 1 torr. Also the quantities of nanofluids that can be produced via this direct-evaporation technique are much more limited than with the two-step method. Nanoparticle agglomeration is minimized as a result of flowing the liquid continuously. Moreover, nanofluids made using this method showed higher conductivity enhancement than the ones made by 2-step method.

1.1 Objectives

When the dimensions of a system are reduced to the nanoscale, the thermal conductivity of the material will decrease due to the boundary scattering of the phonon and/or electrons [13]. It is intuitive that the thermal conductivity of the nanoparticle suspension be lower than that of the large particle suspension. However, measured effective thermal conductivity of nanofluids show higher values than the values calculated by theoretical correlations such as Maxwell [14] and Hamilton-Crosser [15] even when the thermal conductivity of nano-sized particles are taken as a bulk value.

A long list of physical phenomena have been proposed for explaining the experimentally observed enhancement of effective thermal conductivity of nanofluids; including: the size and shape effects, agglomeration, clustering of particles, interfacial resistance, Brownian motion of nanoparticles resulting in micro-convection, phonon dispersion and liquid layering at the particle surface.

In this study, we focus only on the effective thermal conductivity of *stationary* nanofluids, i.e., in the absence of the bulk flow and/or forced or natural convection. The paper is divided into three major parts: i) reviewing the theoretical models, ii) experimental investigations in the open literature, and iii) developing upper/lower bounds for steady-state conduction in stationary nanofluids and comparing them with data. In the experimental part, important phenomena involved in the effective conductivity of nanofluids are discussed and the trends of the data reported are shown.

The objective of this paper is to provide an overview on the important physical phenomena involved in the effective thermal conductivity of nanofluids; and also show the level of scatter and complexity in the published data. The inconsistency seen in the data clearly shows the need for a systematic approach in both experimental and theoretical studies. It also illustrates that the development of a comprehensive model (that can explain all the trends) is a difficult task at the present time.

2 THEORETICAL MODELS

The existing models can be categorized more or less into two general groups [16]:

- *Static* models which assume stationary nanoparticles in the base fluid as a composite in which the thermal transport properties are predicted by conduction-based models such as Maxwell [14] and Hamilton-Crosser [15], etc.
- *Dynamic* models based on the premise that nanoparticles have lateral, random motion in the fluid. This motion is believed to be responsible for transporting energy directly (e.g. through collision between nanoparticles) or indirectly (e.g. micro liquid convection, mixing) that enhances the transport of thermal energy.

The following provides a brief summary of theoretical models.

Using potential theory, Maxwell [14] developed the effective medium theory for non-contacting spherical particles:

$$k^*_{e,\,\mathrm{Maxwell}} = \frac{k^*_p\,(1+2\phi)+2\,(1-\phi)}{k^*_p\,(1-\phi)+(2+\phi)} \qquad (1)$$

where $k^*_p = k_p/k_m$ and $k^*_e = k_e/k_m$. Maxwell's model is valid for relatively small volume fractions. This model has

Copyright © 2006 by ASME

been modified for particle geometry, boundary resistance, and coating [17].

Hamilton and Crosser [15] extended Maxwell's model to include non-spherical particles:

$$k^*_{e,\,\mathrm{HC}} = \frac{k^*_p\left[1+(n-1)\,\phi\right]+(n-1)\,(1-\phi)}{k^*_p\,(1-\phi)+(n-1)+\phi} \qquad (2)$$

where $n = 3/\psi$ and ψ is the sphericity defined as the ratio of the surface area of a sphere, with a volume equal to that of the particle, to the surface area of the particle ($\psi = 1$ for sphere). The parameter n is 3 and 6 for spherical and cylindrical particles, respectively.

Yu and Choi [18; 19] modified the Maxwell and the Hamoilton-Crosser models for the effective thermal conductivity of solid/liquid suspensions to include the effect of *solid layering*. This approach postulates a solid-like layer of liquid on the nanoparticle surface which has a relatively high thermal conductivity compared to the liquid. It is known that liquid molecules close to a solid surface form layered, solid-like structures which may have much higher thermal conductivity compared to the bulk fluid. The existence of this solid layer leads to a larger *effective* volume fraction that can explain the thermal conductivity increase to a certain degree. Yu and Choi [18; 19] concluded that this ordered nanolayer may have an impact on nanofluid thermal conductivity when the particle diameter is less than 10 nm. However, in many cases, a very thick unrealistic solid liquid layer must be assumed to explain the observed enhancements which is unrealistic. Also, temperature dependence of the thermal conductivity of nanofluids cannot be explained by solid layering.

Interfacial thermal resistance exists at the surface interface of liquid and particles. For phonon-based conductors, the interfacial thermal resistance, also known as the Kapitza effect, can arise from differences in the phonon spectra of the two phases, and from scattering at the interface between the phases [11]. The Kapitza effect may be neglected for large-grain sized materials at room temperature. However, for nano-sized structures the interface resistance can play an important role in the overall heat transfer. This resistance will have a *negative* impact on the thermal conductivity of nanofluids.

In *dynamic* models, the Brownian motion [20] of the suspended nanoparticles is assumed to be responsible for the extra thermal conductivity enhancement. Based on Brownian motion theory, the random velocity of the particles is:

$$V \propto \frac{\sqrt{T}}{d_p^{1.5}} \qquad (3)$$

As can be seen in Eq. (3) the particle random velocity has a direct relationship with the square root of the temperature of the mixture and is inversely proportional to the size of the particles to the power 1.5. If the random velocity of the particles is assumed to be responsible for part of the thermal transport in nanofluids, Brownian motion acts in favor of the enhancement observed in nanofluids. The trends predicted by the Brownian motion are qualitatively consistent with the experimental observation in general, i.e., the smaller the size of the particle and the higher the temperature of the nanofluid, the higher the conductivity enhancement. Different ideas have been put forward to explain how Brownian motion contributes to thermal transport e.g., single particle motion, particle-particle collisions, and micro liquid convection [21; 22; 23]. The energy exchange in direct collisions of nanoparticles in nanofluids may result in an enhancement in the effective thermal conductivity. Moreover, thermal conductivity can be enhanced as a result of fluid movement (micro convection) caused by the Brownian motion of nanoparticles. These models, particularly micro convection, are questionable since they assume that the particles are at a temperature different from the liquid. No explanations have been given regarding the origin of this temperature difference. Keblinski et al. [24] (and later Prasher [25]) investigated the effect of the Brownian motion on thermal conductivity of nanofluids and concluded that the thermal diffusion is much faster than Brownian diffusion even for extremely small particles.

Clustering of nanoparticle can result in creating lower thermal resistance paths in the suspension. However, clustering may lead to agglomeration of solids which in turn causes settling down of particles which has a negative effect of conductivity of the suspension. According to Keblinski et al. [24], the percolation threshold for random dispersions is on the order of 15% volume fraction. This rules out the thermal conductivity enhancement of nanofluids in lower volume fractions ($\phi < 5\%$). Another possibility pointed out by [24] is the situation where particles are not in contact, but are within a specific distance (called liquid-mediated) allowing rapid heat flow between them.

Performing an order-of-magnitude analysis, Prasher [25] ruled out other possible mechanisms, and concluded that the convection caused by the Brownian motion is primarily responsible for the enhancement in the thermal conductivity of nanofluids. Prasher [25], following Koo and Kleinstreuer [26] developed a convective-conductive model based on the convection caused by the Brownian motion of nanoparticles and showed good agreement with experimental data collected by others. His model [25]; however, requires two fitting parameters which have relatively large ranges and must be known a priori.

Wang et al. [16] proposed a numerical model for evaluating the contribution of particle Brownian motion coupled with inter-particle electrostatic potential to the thermal energy transport in nanofluids. Their model predicts qualita-

Copyright © 2006 by ASME

tively the trends of the conductivity dependences on particle size, volume fraction, and temperature. They [16] reported that two additional chemical factors, i.e., particle zeta potential and Debye screening length, have strong effects on the thermal conductivity of nanofluids.

In conclusion, the existing models can not predict the trends observed in nanofluids. The answer to the question: which phenomena is responsible for the conductivity enhancement in nanofluids, is still the focus of hot debates in the scientific community.

3 BOUNDS OF CONDUCTION

In this section upper and lower bounds for steady-state heat conduction in liquid-particle mixtures are developed and compared with data. Elrod [27] first introduced these bounds for systems in which conduction is the only mode of heat transfer. The bounds set the limits for the conduction heat transfer in the system. Therefore, the actual thermal conductivity lies between the bounds; often the geometric mean $k_{\text{geometric}} = \sqrt{k_u k_l}$ of the bounds provides a good estimate of the effective thermal conductivity of the system.

The mixture is considered as a large number of cells that can be represented by a basic cell, i.e., a spherical particle in a cube, see Figs. 1 and 2. Thus, the mixture is modelled as identical particles dispersed throughout a continuous medium. Thermal conductivities of the particles and the base fluid are constant, isotropic k_p and k_m, respectively. The boundary conditions of the cell are determined from symmetry and are shown in Fig. 1. The four faces of the cell parallel to the direction of heat flow are adiabatic. The other two faces are isothermal. Heat enters the cell from the top face and exits through the bottom boundary.

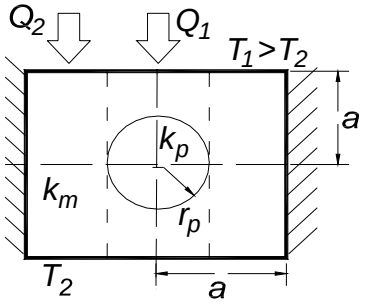

Figure 1. Spherical particle in cubic cell, lower bound: parallel adiabats

3.1 Lower Bound: Parallel Adiabats

A lower bound for the effective conductivity of the basic cell can be established by assuming adiabats parallel to the direction of heat flow, see Fig. 1. Usually particles have much higher thermal conductivities compared to base liquids, i.e., $k_p/k_m >> 1$, thus the thermal resistance of particles may be ignored. In other words, particles can be considered isothermal. This assumption may result in slightly higher values for the conduction bounds, but it will not effect our analysis since we want to establish the bounds for the effective conductivity. It is also a convenient assumption and simplifies the final results.

As shown in Fig. 1, there are two parallel paths in which heat flows Q_1 and Q_2 are being transferred. For a particle of radius r_p in a cubic cell with side dimension, $2a$, after some algebra and normalizing, we find:

$$Q_1 = \frac{\pi \Delta T \; k_m r_p^2}{a} \int_0^1 \frac{\zeta d\zeta}{1 - \phi^* \sqrt{1 - \zeta^2}} \tag{4}$$

where $\Delta T = T_1 - T_2$; $\phi^* = r_p/a$ can be related to the mixture volume fraction

$$\phi^* = \frac{r_p}{a} = \left(\frac{6}{\pi} \phi \right)^{1/3} \tag{5}$$

Equation (4) has a closed form solution

$$Q_1 = -\pi \Delta T \; k_m r_p \frac{\phi^* + \ln(1 - \phi^*)}{\phi^*} \tag{6}$$

The heat transfer through the base fluid can be found from

$$Q_2 = 2a k_m \Delta T \left(1 - \frac{\pi}{4} \phi^{*2} \right) \tag{7}$$

Combining Q_1 and Q_2, the total heat transfer in the unit cell can be found. The effective lower bound for conduction becomes

$$k_l^* = \frac{k_l}{k_m} = 1 - \frac{\pi}{4} \phi^{*2} - \frac{\pi}{2} \phi^* - \frac{\pi}{2} \ln(1 - \phi^*) \tag{8}$$

Note that at the limit where $\phi^* = 0$ (no particles), Eq. (8) yields $k_l^* = 1$ as expected.

3.2 Upper Bound: Perpendicular Isotherms

An upper bound for the effective conductivity of the basic cell can be established by assuming isotherms perpendicular to the direction of heat flow through the cell, see Fig. 2. With an approach similar to the lower bound, the upper bound on effective thermal conductivity for the unit cell can be found:

$$k_u^* = \frac{k_u}{k_m} = \frac{1}{1 - \phi^*} \tag{9}$$

Copyright © 2006 by ASME

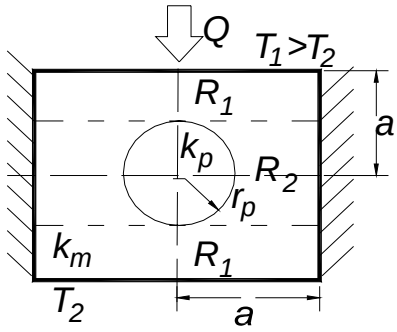

Figure 2. Spherical particle in cubic cell, upper bound: perpendicular isotherms

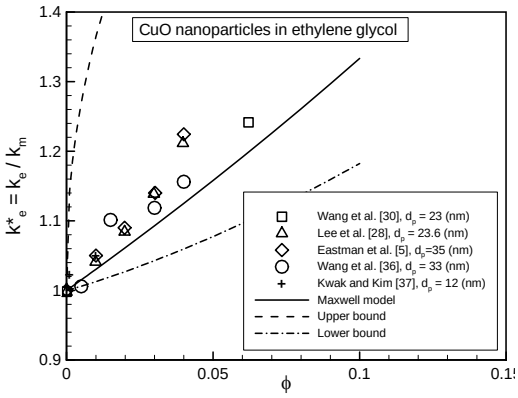

Figure 3. CuO nanoparticles in ethylene glycol, data from various sources.

where at the limit $\phi^* = 0$, Eq. (9) yields $k^*_u = 1$. Applying the same assumption, $k_p/k_m >> 1$, the Maxwell model, Eq. (1) reduces to:

$$k^*_{e,\,\mathrm{Maxwell}}\big|_{k_p/k_m>>1} = \frac{1+2\phi}{1-\phi} \qquad (10)$$

Note that the upper/lower bounds and the Maxwell's model are not sensitive to the conductivity ratio $k^*_p = k_p/k_m$ when k^*_p is about 40 and higher; they approach the isothermal particle case which is being used in the analysis. If the bulk thermal conductivity values can be assumed for the nanoparticles, the thermal conductivity ratio is about 40 or higher for most of the nanofluid data.

3.3 Comparison with Data

Figures 3 to 6 show a comparison between Maxwell's model Eq. (10) and the upper/lower bounds of conduction, i.e., Eqs. (8) and (9) with experimental data. The data are collected from several sources and categorized based on

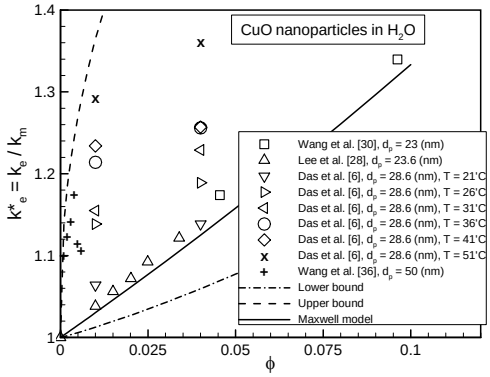

Figure 4. CuO nanoparticles in water, data from various sources.

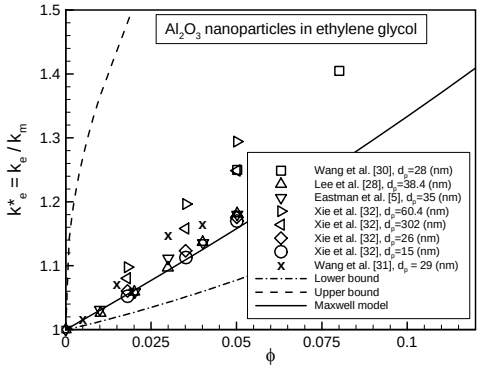

Figure 5. Aluminum oxide nanoparticles in ethylene glycol, data from various sources.

the nanoparticle material and the base fluid which include CuO and Al_2O_3 dispersed in ethylene glycol and water over a range of the volume fraction.

As can be seen in Eqs. (8), (9), and (10), the absolute size of the particles does not have a direct effect on the effective conductivity in conduction-based models; it appears in the volume fraction. However, the nanoparticle diameters (as reported) are listed in Figs. 3 to 6 to show the range of particle sizes used in the tests.

The data show a large scatter, with some level of conductivity enhancement when compared with the Maxwell's model. It is interesting to observe that all the data lies between the lower and upper bounds of conduction.

4 TRENDS IN EXPERIMENTAL DATA

Much experimental research has been performed to study the thermal conductivity enhancement of nanofluid mixtures including nanoparticles Cu, Fe, CuO, CeO_2,

Copyright © 2006 by ASME

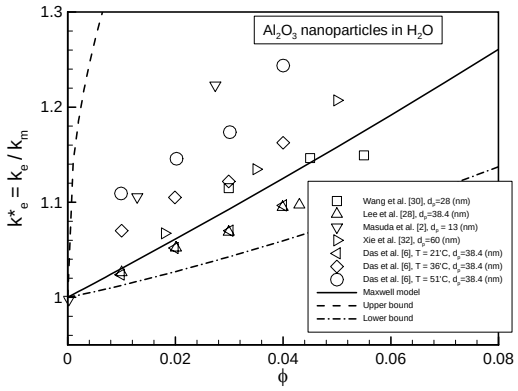

Figure 6. Aluminum oxide nanoparticles in water, data from various sources.

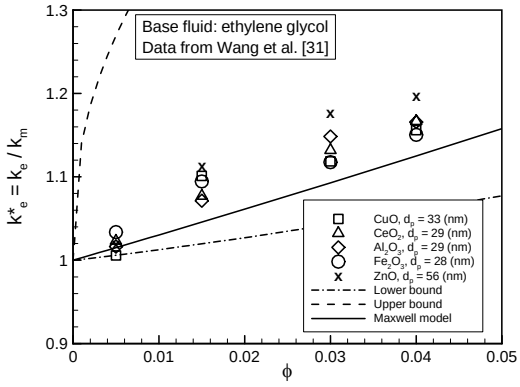

Figure 7. Effect of nanoparticle material on effective thermal conductivity, data [31].

Al_2O_3, ZnO, TiO_2 in base fluids such as water, ethylene glycol and oils. The existing experimental data are collected and summarized in this section. Tables 1 and 2 list reference, particle material, particle size, volume fraction ϕ, base fluid and the maximum conductivity enhancement measured for nanofluids. We also included major findings and important trends reported by researchers in these Tables. For example, the second row of Table 1 reads: Lee et al. [28] used Al_2O_3 and CuO nanoparticles of diameters 38.4 and 23.6 (nm) dispersed in water (H_2O) and ethylene glycol (EG), made suspensions with volume fractions within the range $0 \leq \phi \leq 5\%$, maximum thermal conductivity enhancement measured with $Al_2O_3-H_2O$ and $CuO-H_2O$ were 10% and 12%, respectively.

There are two popular techniques for measuring effective thermal conductivity of nanofluids:

- The *transient hot-wire* (THW) method [29] which involves a wire suspended symmetrically in a liquid in a vertical cylindrical container. The wire serves as both a heating element and a temperature sensor. The THW method is fast and eliminates natural convection effects, this method has been used by a majority of researchers.
- The *steady-state* method (SSM), used by [30; 31], is based on steady-state, one-dimensional heat transfer from an electrical heater to a cold plate through two calibrated heat flux meters. To avoid bulk fluid movement due to natural convection forces, the heat transfer direction should be from top to bottom of the sample.

In the following sub-sections, major trends observed in experimental studies are discussed and when possible the data are shown.

4.1 Effect of Nanoparticles Material

Wang et al. [31] measured thermal conductivity of different nanoparticles including: Al_2O_3, ZnO, CuO, CeO_2, Fe_2O_3 suspended in transformer oil and ethylene glycol. A steady-state method was employed. They also did not use surfactant in their samples. Figure 7 shows comparison between the data of [31] and Maxwell's model and the upper/lower bounds. It is expected to see the highest conductivity enhancement for the nanoparticles which have the highest thermal conductivity (say CuO) and/or the smallest particle size, i.e., Fe_2O_3, see Table 1. However, as shown in Fig. 7, none of the above is true in [31] data. The highest enhancement belongs to ZnO nanoparticles which has the largest mean size of nanoparticles.

Eastman et al. [5] showed that higher thermal conductivity particles result in higher thermal enhancement of the suspension, i.e., the Cu-EG nanofluid had higher thermal conductivity enhancement compared to CuO-EG and Al_2O_3-EG nanofluids. It should be mentioned that Eastman et al. [5] employed a single-step procedure to fabricate their nanofluid samples.

4.2 Shape Effect

Murshed et al. [34] measured the effective thermal conductivity of rod-shapes 10 nm x 40 nm (diameter by length) and spherical shapes of 15 nm TiO_2 nanoparticles in deionized water. A transient hot-wire apparatus was used for the thermal conductivity measurements. As shown in Fig. 8, the cylindrical particles presents a higher enhancement which is consistent with theoretical prediction, i.e., Hamilton-Crosser [15] model. Their experiments [34] also showed a nonlinear relationship between the thermal conductivity and volume fraction at lower volumetric loading (0.005–0.02) and a linear relationship at higher volumetric

Copyright © 2006 by ASME

Table 1. Summary of experimental data: linear increase in conductivity enhancement with volume fraction.

Ref.	Particle	$d_p\,(nm)$	ϕ	Base fluid & $k_e^*\|_{\max}\%$	Notes
[30]	Al_2O_3 CuO	28 23	$0 \le \phi \le 15\%$	H_2O 15 EG 40 engine oil 30 vac. p. fluid 20	viscosity $\nearrow$ as $\phi \nearrow$ k_e^* linear with ϕ SSM, 2-step room T, 3% err
[28]	Al_2O_3 CuO	38.4 23.6	$0 \le \phi \le 5\%$	Al_2O_3 CuO H_2O 10 12 EG 18 22	k_e^* linear with ϕ THW, 2-step room T, 1.5%err $k_e^* \nearrow$ as $d_p \searrow$
[5]	Al_2O_3 Cu CuO	35 10 35	$0 \le \phi \le 5\%$ $0 \le \phi \le 0.5\%$ $0 \le \phi \le 5\%$	EG Cu 40 CuO 22 Al_2O_3 18	k_e^* linear with ϕ THW, **1-step** room T,1.5% err higher k_p higher k_e
[32]	Al_2O_3	15 26 60.4 302	$0 \le \phi \le 5\%$	$d_p = 60(nm)$ EG 31 H_2O 21 pump oil 39	k_e^* linear with ϕ THW, 2-step optimum d_p for k_e^* $k_e^* \searrow$ as pH $\nearrow$ $k_e^* \nearrow$ as $k_p \searrow$
[6]	Al_2O_3 CuO	38.4 28.6	$0 \le \phi \le 4\%$	H_2O@51°C Al_2O_3 25 CuO 35	k_e^* linear with ϕ vari. flx test, 2-step $21 \le T \le 51°C$ $d(k_e/k_m)/dT \nearrow$ as $\phi \nearrow$ $k_e^* \nearrow$ as $T \nearrow$
[31]	Al_2O_3 CeO_2 TiO_2 CuO Fe_2O_3 ZnO	29 29 40 33 28 56	$0 \le \phi \le 4\%$	EG/ 20	k_e^* linear with ϕ SSM no surfactant room T
[33]	Au Ag	$10-20$ $60-80$	$0 \le \phi \le 0.01\%$	thiolate 9 citrate 8.5	k_e^* linear with ϕ vari. flx test, 2-step $30 \le T \le 60°C$ size effect dominates $k_e^* \nearrow$ as $T \nearrow$

Copyright © 2006 by ASME

Table 2. Summary of experimental data: non-linear increase in conductivity enhancement with volume fraction.

Ref.	Particle	$d_p\,(nm)$	ϕ	Base fluid & $k^*\|_{\max}$%	Notes
[34]	TiO_2 sph. TiO_2 cyl.	15 10×40	$0 \le \phi \le 5\%$	H_2O sph. 30 cyl. 33	k_e^***NOT** linear ϕ THW, 2-step room T
[35]	Fe	10 (7.6)	$0 \le \phi \le 0.6\%$	EG/ 18	k_e^***NOT** linear ϕ THW, 2-step, room T $k_e^* \nearrow$ as sonic. t $\nearrow$ higher $k_p \neq$ higher k_e
[36]	CuO	50	$0 \le \phi \le 0.6\%$	H_2O/ 17	k_e^***NOT** linear ϕ quasi-steady state room T
[9]	c. nanotube	$25 \times 50,000$	$0 \le \phi \le 1\%$	α-olefin/ 250	k_e^***NOT** linear ϕ THW, 2-step room T
[37]	CuO	12	$0 \le \phi \le 1\%$	EG/ 6	k_e^***NOT** linear ϕ THW, 2-step Optimum sonic. time room T, prolate sph.

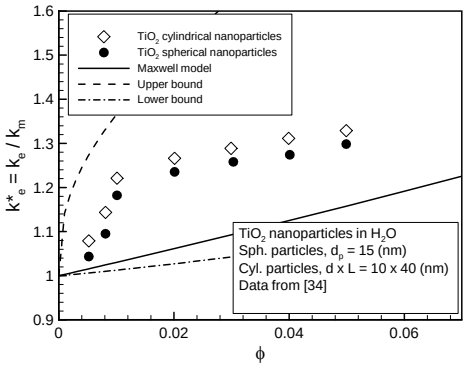

Figure 8. Shape effect: cylindrical and spherical TiO2 nanoparticles in deionized water, data from Murshed et al. [34].

loading (0.02–0.05). They attributed this trend to the influence of the CTAB surfactant and long time (8–10 hours) of sonication, and hydrophobic surface forces in the nanofluids.

4.3 Temperature Effect

Das et al. [6] measured effective thermal conductivities of Al_2O_3 and CuO nanoparticles in water when the mixture temperature was varied between 21 to 51°C. A temperature oscillation technique has been used for the conductivity measurements with a maximum error on the order of 7% at 50°C. They reported a 2 to 4 fold thermal conductivity enhancement of nanofluids over a temperature range of 21°C to 51°C. Also it has been observed that nanofluids containing smaller CuO particles show more enhancement of conductivity with temperature, see Figs. 9 and 10.

4.4 Effect of Sonication Time

Kwak and Kim [37] studied the rheological properties and thermal conductivity enhancement of CuO-ethylene glycol nanofluids with particle size of 10-30 nm. Using Transmission Electron Microscopy (TEM) images, they observed that individual CuO particles have the shape of prolate spheroid of the aspect ratio of 3 and most of the particles are under aggregated states even after sonication for a prolonged period. To disperse particles, sonication was

Copyright © 2006 by ASME

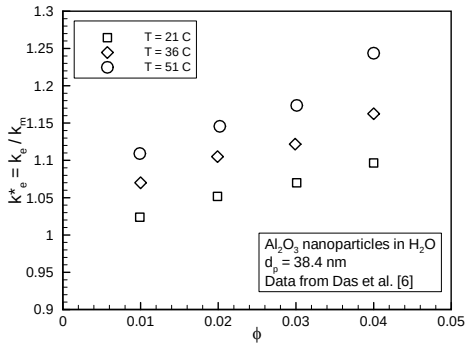

Figure 9. Temperature effect: alumina-water nanofluid, data from Das et al. [6].

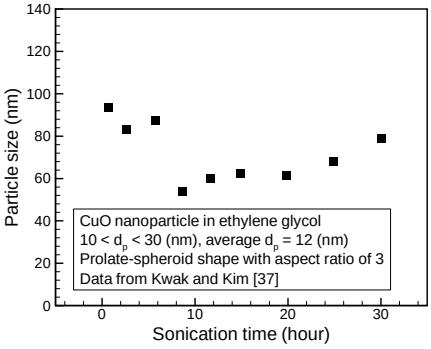

Figure 11. Effect of sonication time on average size of CuO nanoparticle, data from [37].

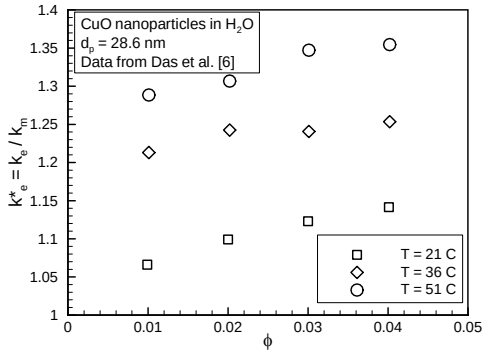

Figure 10. Temperature effect: copper-oxide-water nanofluid, data from Das et al. [6].

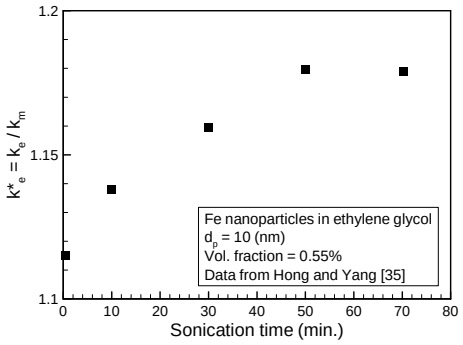

Figure 12. Effect of sonication time on effective thermal conductivity of Fe nanoparticles in ethylene glycol, data from Hong et al. [35].

used with an ultrasound generator (20 kHz, 100W). It was found that if the duration of sonication is too long particles get coalesced again. To determine the optimum duration of sonication, they varied the duration from 1 to 30 hours and measured the average size of particles as shown in Fig. 11. They concluded that the optimum duration time is 9 hours and the average value is approximately 60 nm.

Hong et al. [35] reported that the sonication (with high-powered pulses) results in an improvement in the effective thermal conductivity of nanofluid. Fe-ethylene glycol nanofluids were tested. Thermal conductivity of nanofluids were measured using a transient hot wire method. They measured thermal conductivity of nanofluids while changing the sonication time from 10 up to 70 mins. As shown in Fig. 12, the thermal conductivity increases nonlinearly with the sonication time.

4.5 Particle Size Effect

Xie at al. [32] also measured the effective thermal conductivity of nanofluids (Al_2O_3 in ethylene glycol) with different nanoparticle sizes. They reported an almost linear increase in conductivity with the volume fraction, but the rates of the enhanced ratios to the volume fraction depend on the dispersed nanoparticles. They stated that the enhancements of the thermal conductivities are dependent on Specific Surface Area (SSA) and the mean free path of nanoparticles and the base fluid. Unexpectedly the data do not indicate the highest enhancement for the smallest size nanoparticles as it was expected, see Fig. 13. Xie at al. [32] concluded that the conductivity enhancement is thoroughly different from the traditional suspensions with μm or mm size particles dispersed in a fluid.

Copyright © 2006 by ASME

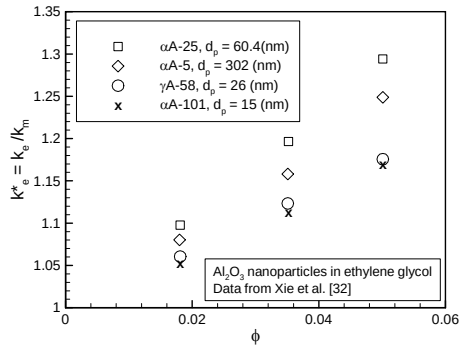

Figure 13. Thermal conductivity enhancement in nanofluids with different particle sizes, data from Xie at al. [32].

4.6 Other Effects

Xie et al. [32] experimentally studied the effect of the pH value of Al_2O_3 nanoparticle in deionoized water. The nanofluid was prepared with a two-step method. The nanoparticles (Al_2O_3) were deagglomerated by intensive ultrasonication after being mixed with a base fluid, and then the suspensions were homogenized by magnetic force agitation [32]. Xie et al. used a transient hot wire technique to measure the thermal conductivity of the suspensions. Their study shows that the effective thermal conductivities of nanofluid increase with an increase in the volume fraction, but with different slope for different pH values. Their results presented in Fig. 14 indicate that the enhanced thermal conductivity ratio decreases with an increase in pH value.

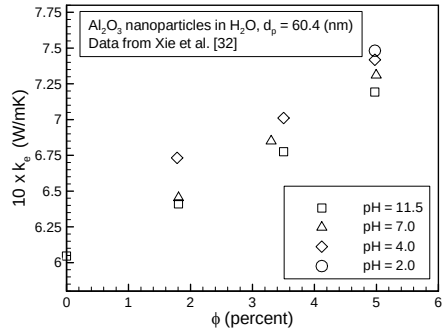

Figure 14. Enhanced thermal conductivity ratio decreases with increasing pH value, data from Xie et al. [32].

There are other effects such as effect(s) of surfactants, Eastman et al. [5] used thioglycolic acid stabilizing agent and reported that the nanofluid samples which included the acidic agents showed improved enhancement comparing with nonacid-containing nanofluids. Particle surface treatment is also believed to have an impact on thermal conductivity of nanofluids.

5 SUMMARY AND CONCLUSIONS

The effective thermal conductivity of stationary nanofluids is studied. A comprehensive review is conducted and the theoretical models and experimental investigations in the open literature are collected and discussed. Our review on theoretical models indicates that a clear understanding of the main mechanism(s) involved in thermal transport phenomena in nanofluids is not established yet.

A review of experimental studies clearly shows a relatively large chaos and randomness in the published data. This requires a careful, repeatable, systematic approach to the thermal conductivity measurement and sample preparation. Only through collecting reliable data can a better understanding of the phenomena in nanofluids be possible. The following summarizes our observations:

- The data show a large scatter; however, they show some level of thermal conductivity enhancement when compared with existing models such as Maxwell's [14].
- Assuming isothermal nanoparticles, we have developed upper/lower bounds for steady-state conduction in stationary nanofluids and compared these bounds with the data. The comparison indicates that the data lies between the bounds of conduction.
- All the tests performed at room temperature, except for Das et al. [6] and [33] in which the effect of temperature on thermal conductivity enhancement has been investigated
- Except for Cu−EG nanofluids used by Eastman et al. [5], where a single-step processed was used, the rest of nanofluids were made using a two-step method
- There is no common trend in thermal conductivity enhancement with increasing the volume fraction. From conduction-based models, it is intuitively expected to see a linear increase in thermal conductivity with volume fraction. However; several groups reported a nonlinear trend, see Murshed et al. [34], Hong et al. [35], Wang et al. [36], and Kim and Kwak [37] (Table 2)
- The effect of nanoparticle size on the effective conductivity is not consistent with data from different groups. The data of [31] and [32] show that there are no direct correlations between the particle size and the effective conductivity enhancement.
- The thermal conductivity of nanoparticles (bulk value) do not seem to have a direct impact on the conductivity enhancement, see the data of [31] and [32]. On

Copyright © 2006 by ASME

the other hand Eastman et al. [5] reported higher thermal conductivity particles results in higher thermal enhancement.

ACKNOWLEDGMENT

The authors gratefully acknowledge the financial support of the Centre for Microelectronics Assembly and Packaging, CMAP and the Natural Sciences and Engineering Research Council of Canada, NSERC.

REFERENCES

[1] S. Choi, "Enhancing thermal conductivity of fluids with nanoparticles," *In Development and Applications of Non-Newtonian Flows, Ed. D A Siginer, H P Wang, pp. 99-105. New York: ASME*, 1995.

[2] H. Masuda, A. Ebata, K. Teramae, and N. Hishinuma, "Alteration of thermal conductivity and viscosity of liquid by dispersing ultra-fine particles (dispersion and al2o3, sio2, and tio2 ultra-fine particles)," *Netsu Bussei (Japan)*, vol. 7, no. 4, pp. 227–233, 1993.

[3] R. G. C. Artus, "Measurements of the novel thermal conduction of a porphoritic heat sink paste," *IEEE Transactions on Components, Packaging, and Manufacturing-Part B*, vol. 19, no. 3, pp. 601–604, 1996.

[4] J. A. Eastman, S. U. S. Choi, S. Li, L. J. Thompson, and S. Lee, "Enhanced thermal conductivity through the development of nanofluids," *Material Research Soceity Symposium Proceedings, Pittsburgh, PA*, vol. 457, pp. 3–11, 1997.

[5] J. A. Eastman, S. U. S. Choi, S. Li, W. Yu, and L. J. Thompson, "Anomalously increased effective thermal conductivities of ethylene glycol-based nanofluids containing copper nanoparticles," *Applied Physics Letters*, vol. 78, no. 6, pp. 718–720, 2001.

[6] S. K. Das, N. Putra, P. Thiesen, and W. Roetzel, "Temperature dependence of thermal conductivity enhancement for nanofluids," *J. of Heat Transfer*, vol. 125, pp. 567–574, 2003.

[7] Z. S. Hu and J. X. Dong, "Study on antiwear and reducing friction factor additive of nanometer titanium oxide," *Wear*, vol. 216, pp. 92–96, 1998.

[8] S. M. You, J. H. Kim, and K. H. Kim, "Effect of nano-particles on critical heat flux of water in pool boiling heat transfer," *Applied Physics Letter*, vol. 83, pp. 3374–3376, 2003.

[9] S. U. S. Choi, Z. G. Zhang, F. E. Lockwood, and E. A. Grulke, "Anomalous thermal conductivity enhancement in nanotube suspensions," *Applied Physics Letters*, vol. 79, pp. 2252–2254, 2001.

[10] B. C. Pak and Y. Cho, "Hydrodynamic and heat transfer study of dispersed fluids with submicron metallic oxide particles," *J. of Experimental Heat Transfer*, vol. 11, no. 2, pp. 151–170, 1998.

[11] J. A. Eastman, S. R. Phillpot, S. U. S. Choi, and P. Keblinski, "Thermal transport in nanofluids," *Annu. Rev. Mater. Res.*, vol. 34, pp. 219–246, 2004.

[12] S. Yatsuya, Y. Tsukasaki, K. Mihama, and R. Uyeda, "Preparation of extremely fine particles by vacuum evaporation onto a running oil substrate," *J. of Crystal Growth*, vol. 45, pp. 490–495, 1978.

[13] K. E. Goodson, M. I. Flik, L. Su, and D. A. Antoniadis, "Prediction and measurement of the thermal conductivity of amorphous dielectric layers," *J. of Heat Transfer*, vol. 116, pp. 317–324, 1994.

[14] J. C. Maxwell, *A Treatise on Electricity and Magnetism*. Oxford, NY, UK: Oxford: Clarendon, 1873.

[15] R. Hamilton and O. K. Crosser, "Thermal conductivity of heterogeneous two-component systems," *IEC Fund.*, vol. 1, no. 3, pp. 187–191, 1962.

[16] J. Wang, G. Chen, and Z. Zhang, "A model of nanofluids thermal conductivity," *Proceedings of ASME Summer Heat Transfer Conference, San Francisco, CA, July 17-22*, 2005.

[17] J. Felske, "Effective thermal conductivity of composite spheres in a continuous medium with contact resistance," *Int. J. of Heat and Mass Transfer*, vol. 47, pp. 3453–3461, 2004.

[18] W. Yu and S. U. S. Choi, "The role of interfacial layers in the enhanced thermal conductivity of nanofluids: A renovated maxwell model," *J. of Nanoparticle Research*, vol. 5, pp. 167–171, 2003.

[19] W. Yu and S. U. S. Choi, "The role of interfacial layers in the enhanced thermal conductivity of nanofluids: A renovated hamilton-crosser model," *J. of Nanoparticle Research*, vol. 6, pp. 355–361, 2004.

[20] G. E. Uhlenbeck and L. S. Ornstein, "On the theory of the brownian motion," *Physical Review*, vol. 36, 1930.

[21] Y. Xuan, Q. Li, and W. Hu, "Aggregation structure and thermal conductivity of nanofluids," *AIChE Journal*, vol. 49, no. 4, 2003.

[22] S. Jang and S. U. S. Choi, "Role of brownian motion in the enhanced thermal conductivity of nanofluids," *Applied Physics Letters*, vol. 84, no. 21, pp. 4316–4318, 2004.

[23] D. H. Kumar, H. E. Patel, V. R. R. Kumar, T. Sundarajan, T. Pradeep, and S. K. Das, "Model for heat conduction in nanofluids," *Physical Review Letters*, vol. 93, no. 14, pp. 144301–144305, 2004.

[24] P. Keblinski, S. R. Phillpot, S. U. S. Choi, and J. A. Eastman, "Mechanisms of heat flow in suspensions of nano-sized particles (nanofluids)," *Int. J. of Heat and*

Copyright © 2006 by ASME

Mass Transfer, vol. 45, pp. 855–863, 2002.

[25] R. Prasher, "Brownian-motion-based convective model for the thermal conductivity of nanofluids," *Proceedings of ASME Summer Heat Transfer Conference, San Francisco, CA, July 17-22*, 2005.

[26] J. Koo and C. Kleinstreuer, "A new thermal conductivity model for nanofluids," *J. of Nanoparticle Research*, vol. 6, pp. 577–588, 2005.

[27] H. G. Elrod, "Two simple theorems for establishing bounds on the total heat flow in steady-state heat-conduction problems with convective boundary conditions," *J. of Heat Transfer*, vol. 96, no. 1, pp. 65–70, 1994.

[28] S. Lee, S. U. S. Choi, S. Li, and J. A. Eastman, "Measuring thermal conductivity of fluids containing oxide nanoparticles," *J. of Heat Transfer*, vol. 121, pp. 280–289, 1999.

[29] Y. Nagasaka and A. Nagashima, "Absolute measurement of the thermal conductivity of electrically conducting liquids by transient hot-wire method," *J. Phys. E: Sci. Instrum.*, vol. 14, pp. 1435–1439, 1981.

[30] X. Wang, X. Xu, and S. U. S. Choi, "Thermal conductivity of nanoparticle-fluid mixture," *J. of Thermophysics and Heat Transfer*, vol. 13, no. 4, pp. 474–480, 1999.

[31] Y. Wang, T. S. Fisher, J. L. Davidson, and L. Jiang, "Thermal conductivity of nanoparticle suspensions," *8th AIAA and ASME Joint Thermophysics and Heat Transfer Conf., St. Louis, 24-26 June*, 2002.

[32] H. Xie, J. Wang, T. Xi, Y. Liu, and F. Ai, "Thermal conductivity enhancement of suspensions containing nanosized alumina particles," *J. of Applied Physics*, vol. 91, no. 7, pp. 4568–4572, 2002.

[33] H. E. Patel, S. K. Das, T. Sundararajan, A. Sreekumaran, B. George, and T. Pradeep, "Thermal conductivity of naked and monolayer protected metal nanoparticle based nanofluids: Manifestation of anomalous enhancement and chemical effects," *Applied Physics Letters*, vol. 83, no. 14, 2003.

[34] S. M. S. Murshed, K. C. Leong, and C. Yang, "Enhanced thermal conductivity of tio2-water based nanofluids," *Int. J. of Thermal Science*, vol. 44, pp. 367–373, 2005.

[35] T. Hong, H. Yang, and C. J. Choi, "Study of the enhanced thermal conductivity of fe nanofluids," *J. of Applied Physics*, vol. 97, pp. 064311–1–064311–4, 2005.

[36] B. Wang, L. Zhou, and X. Peng, "A fractal model for predicting the effective thermal conductivity of liquid with suspension of nanoparticles," *Int. J. of Heat and Mass Transfer*, vol. 46, pp. 2665–2672, 2003.

[37] K. Kwak and C. Kim, "Viscosity and thermal conductivity of copper oxide nanofluid dispersed in ethylene glycol," *Korea-Australia Rheology Journal*, vol. 17, no. 2, 2005.

Copyright © 2006 by ASME